Structural Investigation of the Metallic Glasses $Mg_{85.5}Cu_{14.5}$ and $Mg_{70}Zn_{30}$

E. Nassif*, P. Lamparter, W. Sperl, and S. Steeb
Max-Planck-Institut für Metallforschung, Institut für Werkstoffwissenschaften Stuttgart, Germany

Z. Naturforsch. **38 a,** 142–148 (1983); received September 30, 1982

Dedicated to Professor Alfred Klemm on the occasion of his 70th birthday

The total structure factors as well as the total pair correlation functions for amorphous $Mg_{85.5}Cu_{14.5}$ (by neutron and X-ray diffraction) and for amorphous $Mg_{70}Zn_{30}$ (by X-ray diffraction) were determined. Both alloys show similar chemical short range order effects. From the total pair correlation function of the $Mg_{85.5}Cu_{14.5}$ glass, partial coordination numbers and atomic distances could be extracted. Comparison with the structure of crystalline Mg_2Cu suggests that the short range order around the copper atoms is similar in the amorphous and the crystalline phase. The densities of both amorphous alloys were measured yielding negative excess volumina.

Introduction

Metallic glasses can be classified into five different classes: T-M, T-T, T-B, R-B, B-B, where T, M, B, R mean transition metal, metalloid, simple metal, and rare earth metal, respectively. While for the first three classes many structural investigations have been performed, for the last two classes only few studies have been done up to now. It has been proved that all metallic glasses investigated so far exhibit more or less pronounced chemical short range order (CSRO). It was of interest to examine whether metallic glasses belonging to the B-B group also show a CSRO effect. In the present work the structure of amorphous $Mg_{85.5}Cu_{14.5}$ has been studied by X-ray- and neutron-diffraction, and the structure of amorphous $Mg_{70}Zn_{30}$ by X-ray diffraction. For amorphous Mg-Zn several investigations can be found in literature [1, 2], whereas a diffraction study on Mg-Cu metallic glasses produced by the melt spinning technique is reported here for the first time to our knowledge.

Theoretical Basis

In the following the equations needed in the present study will be given. For a comprehensive description see e.g. [3].

The total structure factor $S^{FZ}(Q)$ according to the Faber Ziman definition [4] is

$$S^{FZ}(Q) = [I_C(Q) - \text{LMS}]/\langle f \rangle^2, \qquad (1)$$

where

Q $= 4\pi(\sin\theta)/\lambda$ = absolute value of the scattering vector $\boldsymbol{Q}$,
2θ = scattering angle,
λ = wavelength of the radiation,
$\langle f \rangle$ $= c_1 f_1 + c_2 f_2$,
c_1, c_2 = molar fraction of the constituent 1, 2,
f_1, f_2 = scattering factor of the constituent 1, 2, which depends on Q for the case of X-rays,
$I_C(Q)$ = coherently scattered intensity per atom,
LMS $= \langle f^2 \rangle - \langle f \rangle^2$ = Laue monotonic scattering.

The total pair correlation function $G(R) = 4\pi R^2[\varrho(R) - \varrho_0]$ is obtained by Fourier transformation of $S^{FZ}(Q)$:

$$G(R) = \frac{2}{\pi} \int_0^{Q_m} Q\,[S^{FZ}(Q) - 1] \sin(QR)\,\mathrm{d}Q. \qquad (2)$$

$\varrho(R)$ is the atomic number density at distance R from a reference atom, ϱ_0 the mean atomic number density, and Q_m the maximum experimental Q-value.

The coordination number N^I is calculated from the radial distribution function $\text{RDF} = 4\pi R^2 \varrho(R)$ according to:

$$N^I = \int_{R_l}^{R_u} \text{RDF}(R)\,\mathrm{d}R\,, \qquad (3)$$

where the lower and upper integration limits R_l and R_u refer to the minima preceding and following the main peak of the RDF, respectively. $G(R)$ can be

---

* Permanent address: University of Buenos Aires, Engineering Faculty, Department of Physics, Paseo Colon 850, 1063 Buenos Aires, Argentine

Reprint requests to Prof. Dr. S. Steeb, Max-Planck-Institut für Metallforschung, Institut für Werkstoffwissenschaften, Seestraße 92, 7000 Stuttgart.

0340-4811 / 83 / 0200-0142 $ 01.3 0/0. – Please order a reprint rather than making your own copy.

expressed in terms of the three partial pair correlation functions $G_{ij}(R)$:

$$G(R) = \frac{c_1^2 f_1^2}{\langle f\rangle^2} G_{11}(R) + \frac{c_2^2 f_2^2}{\langle f\rangle^2} G_{22}(R) + \frac{2\, c_1 c_2 f_1 f_2}{\langle f\rangle^2} G_{12}(R)\,, \tag{4}$$

where $G_{ij}(R)$ represents the distribution of j-type atoms around an i-type atom. It is related to the corresponding partial distribution function $\varrho_{ij}(R)$ according to

$$G_{ij}(R) = 4\pi\, R[\varrho_{ij}(R)/c_j - \varrho_0]\,. \tag{5}$$

The partial coordination numbers Z_{ij} are calculated from the $\varrho_{ij}(R)$ analogously to (3).

An alternative description of the structure of binary amorphous alloys can be given in terms of the three partial Bhatia Thornton structure factors [5]:

$$\begin{aligned} S^{\mathrm{BT}}(Q) &= \frac{I_{\mathrm{C}}(Q)}{\langle f^2\rangle} \\ &= \frac{\langle f\rangle^2}{\langle f^2\rangle} S_{\mathrm{NN}}(Q) + \\ &\quad + \frac{c_1 c_2 (f_1 - f_2)^2}{\langle f^2\rangle} S_{\mathrm{CC}}(Q) \\ &\quad + \frac{2\langle f\rangle (f_1 - f_2)}{\langle f^2\rangle} S_{\mathrm{NC}}(Q)\,. \end{aligned} \tag{6}$$

$S_{\mathrm{NN}}(Q)$ is the structure factor of the correlations between density fluctuations. It describes the topological ordering in the amorphous system. $S_{\mathrm{CC}}(Q)$ is the structure factor of the correlations between concentration fluctuations. It represents the chemical short range ordering. $S_{\mathrm{NC}}(Q)$ is the structure factor of the cross correlations. It shows up the so called size effect and equals zero for the case of equal sized components.

Experimental

Sample Preparation

The $Mg_{85.5}Cu_{14.5}$ and $Mg_{70}Zn_{30}$ alloys were carefully prepared by alloying the components under argon atmosphere to avoid oxygen contamination.

The amorphous samples were obtained by means of the melt spinning technique (see e.g. Ref. [6]) under helium atmosphere as ribbons, 1 mm wide and 0.025 mm thick in case of $Mg_{85.5}Cu_{14.5}$ and 1 mm wide and 0.020 mm thick for $Mg_{70}Zn_{30}$. The density D of the samples was measured by the liquid displacement method [7] using acetone. The measured values are listed in Table 1.

Table 1. D = density, d_i = atomic diameter [8], Q^{P}, Q^{I} = position of the prepeak and the main peak, respectively, of the X-ray structure factor. ΔQ^{P}, ΔQ^{I} = widths of the peaks, I^{P} = amplitude of the prepeak.

	$Mg_{85.5}Cu_{14.5}$	$Mg_{70}Zn_{30}$
D [g/cm³]	2.54	3.08
excess volume	– 10%	– 5.3%
$d_{\mathrm{Mg}}/d_{\mathrm{Cu}}$; $d_{\mathrm{Mg}}/d_{\mathrm{Zn}}$	3.20/2.56 = 1.25	3.20/2.76 = 1.16
Q^{P} [Å^{-1}]	1.48	1.54
Q^{I} [Å^{-1}]	2.65	2.65
ΔQ^{P} [Å^{-1}]	0.83	0.78
ΔQ^{I} [Å^{-1}]	0.34	0.44
I^{P}	0.279	0.272
$Q^{\mathrm{P}}/Q^{\mathrm{I}}$	0.56	0.58

X-Ray-Diffraction

For the preparation of the specimens for the transmission technique, parallel aligned ribbons were mounted on an aluminum frame. In order to obtain a reasonable scattered intensity three layers of these ribbons were taken. The X-ray measurements were performed in a D-500 Siemens diffractometer in transmission mode. The diffractometer consists of a stationary line focus X-ray tube (Mo-Target, $\lambda_{\mathrm{K}\alpha} = 0.71$ Å), a specimen table which rotates at one-half the angular speed of the detector arm, and a scintillation-crystal detector. To prevent air-scattered radiation, all the measurements have been done under vaccum. Diffraction patterns were recorded within a 2θ-range from 3° to 108° with 0.1° step scan width.

The measuring time per scan was 18 h. A pair of filters consisting of yttrium (150 μm thick) and zirconium (90 μm thick), respectively was used following the Ross-filter method [9] where one separate scan was carried out with each filter.

The measured data were collected in a multichannel analyzer and transferred to a central computer after each scan. The intensities obtained with each filter were subtracted from each other, giving as result a diffracted intensity equivalent to that normally obtained using monochromatic radiation. The resolution power with this experimental set up was determined to be $\Delta 2\theta = 0.6°$ in the range of the main peak, which is sufficient for diffraction studies with amorphous samples.

As the scattered intensity showed a large amount of fluorescence radiation, produced by the copper and zinc contents of the samples, respectively, an iron foil (18 μm thick) was inserted between sample and detector in order to suppress this low energy part of the radiation. In addition, a narrow setting of the discriminator window was chosen.

After the usual corrections for polarization and absorption [10], the data were normalized following the Krogh Moe method [11]. The scattering factors of the constituents were taken from [12], whereby the values for uncharged atoms were used. The subtraction of the Compton scattering intensity, which was calculated following [13], yielded finally the coherently scattered intensity per atom $I_C(Q)$ from which the structure factor $S^{BT}(Q)$ was calculated according to (6).

Neutron Diffraction

The neutron diffraction experiment with $Mg_{85.5}Cu_{14.5}$ was performed using the D2-diffractometer at the Laue Langevin Institute, Grenoble. The specimen was prepared by cutting the amorphous ribbon into small shreds and pressing them randomly oriented into a vanadium tube with 0.1 mm wall thickness, 42 mm height, and 11.5 mm diameter. The measurements were performed with a neutron wavelength of 1.22 Å in the 2θ-range from 1.4° up to 120° with 0.2° step scan width. Besides the scan with the specimen additional runs with empty diffractometer, empty vanadium container, and with a Cd-rod, having the same dimensions as the sample, were carried out. The corrections for scattering contributions of the background and the container as well as for absorption in the sample and in the container were done according to Paalman and Pings [14]. The corrected intensity data were normalized by the Krogh Moe method [11] to obtain the coherent scattering $I_C(Q)$ per atom. Thereby the multiple scattering correction was done corresponding to [15]. Table 2 shows the neutron scattering and absorption parameters for Mg and Cu used in the present study.

Table 2. Scattering and absorption parameters for neutrons [16, 17]. f = coherent scattering length, σ_{inc} = incoherent scattering cross section, σ_a = absorption cross section.

	f [10^{-12} cm]	σ_{inc} [barn]	σ_a [barn]
Mg	0.538	0.07	0.045
Cu	0.77	0.5	2.49

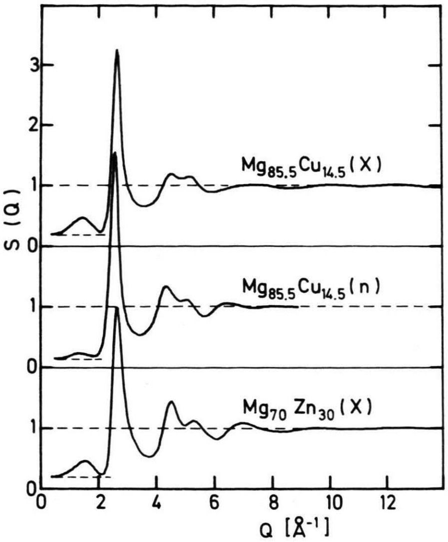

Fig. 1. Total structure factors of amorphous $Mg_{85.5}Cu_{14.5}$ and $Mg_{70}Cu_{30}$.

Results and Discussion

$Mg_{85.5}Cu_{14.5}$

a) Structure Factors

The two upper curves of Fig. 1 show the two total structure factors $S_n^{BT}(Q)$ and $S_X^{BT}(Q)$ of $Mg_{85.5}Cu_{14.5}$ obtained by neutron scattering and by X-ray scattering, respectively. The lower curve of Fig. 1 shows the total structure factor $S_X^{BT}(Q)$ of $Mg_{70}Zn_{30}$. All three curves were calculated from $I_c(Q)$ according to the definition given by (6). It can be noted that a splitting up of the second maximum into two subpeaks occurs also with metallic glasses of the B-B class as was usually observed for other metallic glasses. Especially from the difference between the amplitudes of the main maximum and the second maximum strong damping of the oscillations with rising Q-values can be observed.

The most interesting feature, however, is the occurrence of a prepeak at $Q \cong 1.5$ Å^{-1}, which is very pronounced in the case of the X-ray curve. This prepeak already indicates a marked chemical ordering effect in amorphous $Mg_{85.5}Cu_{14.5}$, which is discussed in the following in terms of the Bhatia Thornton partial structure factors. For the case of

X-rays, (6) becomes

$$S_X^{BT}(Q) = 0.851\, S_{NN}(Q) + 0.146\, S_{CC}(Q) + 2.007\, S_{NC}(Q) \qquad (7)$$

and for neutrons

$$S_n^{BT}(Q) = 0.980\, S_{NN}(Q) + 0.020\, S_{CC}(Q) + 0.787\, S_{NC}(Q)\,. \qquad (8)$$

From the weighting factors in (7) and (8) it is seen that the contribution of $S_{CC}(Q)$ and $S_{NC}(Q)$ is much stronger in the case of X-rays than in the case of neutrons. Therefore from the weighting factors alone it cannot be decided whether the prepeak must be attributed to $S_{NC}(Q)$ o $S_{CC}(Q)$. However, for the following reasons it can be argued that it does not belong to $S_{NC}(Q)$:

i) Figure 2 shows a $S_{NC}(Q)$ model curve which has been calculated with the Ashcroft Lang reth hardsphere model [18], in which, however, chemical ordering effects are not taken into account. $S_{NC}(Q)$ exhibits a negative peak at $Q = 2.5$ Å^{-1} and a negligeable positive contribution at $Q = 1.48$ Å^{-1} where the prepeak in Fig. 1 is positioned. Since the positions of $S_{NC}(Q)$-peaks are mainly determined by the atomic diameters of both constituents, we conclude that even strong CSRO effects cannot modify the $S_{NC}(Q)$ model curve in such a way that it could show a positive peak at $Q = 1.48$ Å^{-1}.

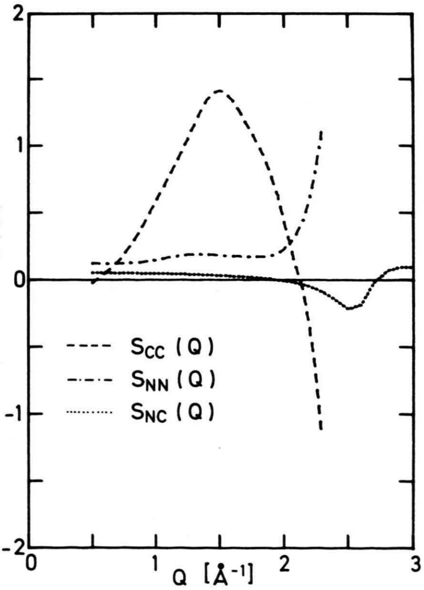

Fig. 2. Partial Bhatia Thornton structure factors of amorphous $Mg_{85.5}Cu_{14.5}$ in the low Q region. $S_{NC}(Q)$ calculated with a hardsphere model. $S_{NN}(Q)$, $S_{CC}(Q)$ calculated from the total structure factors in Figure 1.

ii) The contribution of $S_{NC}(Q)$ disappears if the atomic diameters of the two components are equal. As can be seen in Table 1, the atomic diameter ratio is closer to 1 for the case of Mg-Zn than for the case of Mg-Cu. Therefore the contribution of $S_{NC}(Q)$ to the total structure factor is expected to be smaller in the case of Mg-Zn. On the other hand the amplitudes of the X-ray prepeaks in Fig. 1 are equal for both alloys. This also supports the conclusion that the prepeak has to be attributed to $S_{CC}(Q)$.

For the calculation of the three partial structure factors one needs, in principle, three equations corresponding to (6) that means three independent diffraction experiments. In the present study an attempt was made to calculate the two partial structure factors $S_{NN}(Q)$ and $S_{CC}(Q)$ from (7) and (8) using the hardsphere model curve for $S_{NC}(Q)$. This calculation yielded, however, reliable results for S_{NN} and S_{CC} only in the low Q-region up to 2 Å^{-1}, where the contribution of S_{CC} is large.

In Fig. 1 it can be seen that the width ΔQ^p of the prepeak which belongs to $S_{CC}(Q)$ is larger than the width ΔQ^I of the main peak which belongs to $S_{NN}(Q)$ (compare also Table 1).

A correlation length ξ can be calculated from a width ΔQ according to the Scherrer-formula [19]

$$\xi = 2\pi/\Delta Q\,. \qquad (9)$$

With the experimental data from Table 1 we obtain from ΔQ^p the correlation length $\xi^{CSRO} \cong 8$ Å and from ΔQ^I the correlation length $\xi^{TSRO} \cong 18$ Å. This means that the range of correlation between the concentration fluctuations (Chemical short range order = CSRO) is clearly smaller than that between the density fluctuations (Topological short range order = TSRO). The comparison with the pair correlation function $G(R)$ of Fig. 3 shows that apparently ξ^{TSRO} marks the range in which the amplitudes of the peaks of $G(R)$ are damped below 5% of the main peak amplitude.

b) Atomic Distances and Coordination Numbers

From the Faber Ziman total structure factors $S_X^{FZ}(Q)$ and $S_n^{FZ}(Q)$, the corresponding total pair correlation functions $G_X(R)$ and $G_n(R)$ were calculated using (2). These functions are plotted in Figure 3. They show up the presence of rather extended correlations in amorphous $Mg_{85.5}Cu_{14.5}$ up to at least $R = 25$ Å. From these curves, the radius of

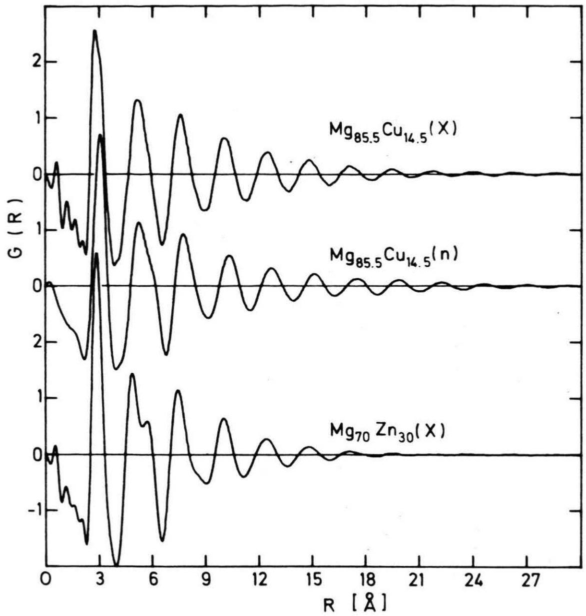

Fig. 3. Total pair correlation functions of amorphous $Mg_{85.5}Cu_{14.5}$ and $Mg_{70}Zn_{30}$. $G_X(R)$ obtained with X-rays. $G_n(R)$ obtained with neutrons.

the first coordination shell R^I was taken. Furthermore, the total coordination number N^I was calculated using (3) (see Table 3). In connection with Table 3 it should be mentioned that the values for R^I and N^I in this Table are not expected to be the same for X-rays and neutrons since R^I as well as N^I depend on the scattering factors as was shown in (4).

In Fig. 4 the first maximum of the $G_X(R)$ curve is magnified and one can see the presence of a pronounced shoulder. According to (4) the total pair correlation function can be expressed in terms of the partial correlation functions as follows:

$$G_X(R) = 0.085\,G_{CuCu}(R) + 0.503\,G_{MgMg}(R) + 0.412\,G_{MgCu}(R)\,. \qquad (10)$$

Table 3. Structural parameters. R^I, N^I = atomic distance and total coordination number, respectively, calculated from the total pair correlation function. R_{ij} = atomic distance, Z_{ij} = partial coordination number of j-type atoms around an i-type atom.

	$Mg_{85.5}Cu_{14.5}$	$Mg_{70}Zn_{30}$
R^I [Å]	2.75 (X-rays) 3.05 (neutrons)	2.88 (X-rays)
N^I	10.2 (X-rays) 11.4 (neutrons)	10.7 (X-rays)
R_{MgMg}; R_{MgCu} [Å]	3.10; 2.71	–
Z_{MgMg}; Z_{MgCu}; Z_{CuMg}	9.6; 1.4; 8.3	–

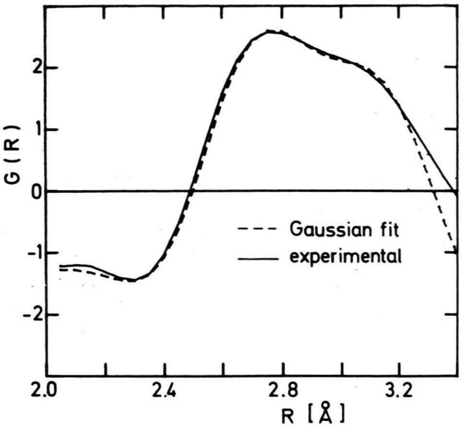

Fig. 4. Main peak of the $G_X(R)$ for amorphous $Mg_{85.5}Cu_{14.5}$. —— experimental; ----- by Gaussian fitting.

From the weighting factors follows that the contribution of the copper-copper correlation function is very small. From this and from the fact that the atomic diameter of magnesium is larger than that of copper we conclude that the first subpeak in Fig. 4 corresponds to the partial $G_{MgCu}(R)$-function, and the second one to the partial $G_{MgMg}(R)$-function. The atomic distances R_{MgMg} and R_{MgCu}, as well as the partial coordination numbers Z_{MgMg} and Z_{MgCu} have been obtained on this basis as follows: The main maximum of the RDF(R)-function corresponding to $G_X(R)$ in Fig. 4 was fitted by the sum of two Gaussians:

$$\mathrm{RDF}(R) = \sum_{L=1}^{2} \frac{N_L}{\sqrt{2\pi}\,\varepsilon_L R_L} \cdot R\left[\exp\left\{\frac{-(R-R_L)^2}{2\varepsilon_L^2}\right\} - \exp\left\{\frac{-(R+R_L)^2}{2\varepsilon_L^2}\right\}\right], \qquad (11)$$

where the position R_L, the width $\sigma_L = 2.355\,\varepsilon_L$ and the area N_L were the fitting parameters. The second term in (11) is introduced for mathematical reasons and is negligible for positive values of R. By Fourier transformation of the RDF(R) of (11) into the Q-space, cutting the transformed function at the maximum Q-value, which was the same as that of the measured structure factor $S_X^{FZ}(Q)$, and then transforming it back to R-space, the model RDF(R)-function was artificially supplied with the same termination effects as the experimental RDF(R).

R_1 and R_2 yield the distances R_{MgCu} and R_{MgMg}, respectively. The partial coordination numbers were calculated from the areas N_L:

$$Z_{\mathrm{MgCu}} = \left[\frac{2\,c_{\mathrm{Mg}} f_{\mathrm{Mg}} f_{\mathrm{Cu}}}{\langle f\rangle^2}\right]^{-1} N_1\,,$$

$$Z_{\mathrm{MgMg}} = \left[\frac{c_{\mathrm{Mg}} f_{\mathrm{Mg}}^2}{\langle f\rangle^2}\right]^{-1} N_2\,, \qquad (12)$$

$$Z_{\mathrm{CuMg}} = \frac{c_{\mathrm{Mg}}}{c_{\mathrm{Cu}}}\, Z_{\mathrm{MgCu}}\,.$$

The corresponding results are listed in Table 3. The atomic distance between Mg atoms corresponds well to the atomic diameter of Mg ($d_{\mathrm{Mg}} = 3.2$ Å) [8], whereas the Mg-Cu distance is smaller than the mean value $\bar{d}$ of the atomic diameters of Mg and Cu

$$\bar{d} = \frac{3.2 + 2.56}{2} = 2.88 \text{ Å}\,.$$

The Gaussian fit is also plotted in Figure 4. The comparison with the experimental curve shows that the run of the latter one is more asymmetric than that of the model curve. As a consequence, the real partial coordination number Z_{MgMg} could be even larger than the value given in Table 3.

The main maximum of the correlation curve $G_n(R)$ obtained by neutron diffraction shows no shoulder and is slightly shifted to larger R-values. This can be explained firstly by the fact that the integration length with the neutron experiment is smaller, leading to a broadening of the maxima in R-space. Secondly, the weighting factor for neutrons in (4) for Mg-Mg is larger and that for Mg-Cu is smaller than the corresponding ones for X-rays which finally leads to a preference of the Mg-Mg-distance in the $G_n(R)$-curve.

c) Comparison with Crystalline Mg_2Cu

It is of interest whether the chemical short range order found in metallic glasses resembles to that of the corresponding crystalline phases. It is known that a crystalline phase Mg_2Cu exists, the structure of which is reported in [20].

Figure 5 shows part of the unit cell where the copper atom is surrounded by 8 magnesium atoms at a mean distance of 2.72 Å forming a distorted hexahedron. These features agree well with the respective values for amorphous $Mg_{85.5}Cu_{14.5}$: $Z_{\mathrm{CuMg}} = 8.3$, $R_{\mathrm{MgCu}} = 2.71$ Å. From these observations one can conclude that the nearest neighbour arrangements around a central Cu-atom in amorphous $Mg_{85.5}Cu_{14.5}$ and crystalline Mg_2Cu are similar. Concerning the surrounding of a central Mg-atom we state a rather large difference in the partial coordination number Z_{MgCu} which amounts to 1.4 atoms in the amorphous phase compared to 4 atoms in the crystalline phase which can be understood by the higher Cu-concentration in the latter case.

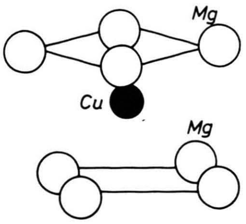

Fig. 5. Part of the unit cell of crystalline Mg_2Cu.

Concerning the Mg-Mg correlation the following should be pointed out: The Mg-Mg distances in crystalline Mg_2Cu are according to [20] distributed rather closely in a first region from 2.91 up to 3.09 Å, and in a second region from 3.31 up to 3.47 Å. Regarding Fig. 4 one may suppose that in the amorphous phase the Mg-Mg distances of those two regions have moved together into the region between 2.90 and 3.20 Å.

$Mg_{70}Zn_{30}$

Figure 1 shows also the total structure factor $S_{\mathrm{X}}^{\mathrm{BT}}(Q)$ of amorphous $Mg_{70}Zn_{30}$ obtained by X-ray diffraction. One can see that the splitting of the second maximum is more pronounced than in the case of amorphous $Mg_{85.5}Cu_{14.5}$. It is of interest to see again the occurrence of a prepeak whose amplitude and width are rather similar to that of $Mg_{85.5}Cu_{14.5}$ and which is also attributed to $S_{\mathrm{CC}}(Q)$.

That means that also in amorphous $Mg_{70}Zn_{30}$ pronounced chemical ordering is present. From the width of the prepeak the correlation length of the CSRO was calculated using (9) yielding $\xi^{\mathrm{CSRO}} \cong 8$ Å.

The structural parameters of $S_{\mathrm{X}}^{\mathrm{BT}}(Q)$ are listed in Table 1. It can be seen that the ratio $Q^{\mathrm{P}}/Q^{\mathrm{I}}$ of the positions of the prepeak and the mainpeak is slightly larger for Mg-Zn than for Mg-Cu.

The amplitude I^{P} of the prepeak is related to the concentration-concentration partial structure factor $S_{\mathrm{CC}}(Q)$ which is a measure of the strength of the

CSRO in the following way:

$$I^{\mathrm{p}} \cong \frac{(\Delta f)^2}{\langle f^2 \rangle} c_1 c_2 S_{\mathrm{CC}}(Q^{\mathrm{p}}) = k\, S_{\mathrm{CC}}(Q^{\mathrm{p}}) , \qquad (13)$$

where the constant k equals 0.146 for Mg-Cu and 0.183 for Mg-Zn. The amplitudes of the prepeak I^{p} were taken from the structure factors as illustrated in Fig. 1 and are listed in Table 1. These values yield with (13):

$$S_{\mathrm{CC}}^{\mathrm{MgCu}}(Q^{\mathrm{p}}) / S_{\mathrm{CC}}^{\mathrm{MgZn}}(Q^{\mathrm{p}}) = 1.3 ,$$

which is a hint for a stronger CSRO in Mg-Cu than in Mg-Zn.

In Fig. 3 the total pair correlation function $G(R)$ calculated from $S^{\mathrm{FZ}}(Q)$ according to (2) is plotted. It exhibits a strong splitting of the second maximum which was not observed in the case of Mg-Cu, and atomic distance correlations up to 20 Å can be observed. On the other hand the first maximum shows no shoulder as for Mg-Cu. This can be attributed to the fact that the difference of the atomic sizes of Mg and Zn is clearly smaller than the difference of the atomic sizes of Mg and Cu. The radius of the first coordination shell R^{I} and the total coordination number N^{I} were taken from the $G(R)$-curve and are listed in Table 3.

Conclusion

The atomic scale structure of the metallic glasses $Mg_{85.5}Cu_{14.5}$ and $Mg_{70}Zn_{30}$ has been investigated by diffraction experiments. It has been shown that metallic glasses of this class, whose constituents are simple metals, show pronounced chemical short range ordering. The X-ray-structure factors of both amorphous alloys exhibit a prepeak which could be attributed to the partial structure factor $S_{\mathrm{CC}}(Q)$ of the correlation between the concentration fluctuations. From the large width of the prepeak compared to the width of the main peak of the total structure factors, rather restricted spatial extension for the CSRO (only up to 8 Å) was concluded. Comparison of the amplitude of the $S_{\mathrm{CC}}(Q)$ peaks suggests that the CSRO is stronger in amorphous $Mg_{85.5}Cu_{14.5}$ than in the $Mg_{70}Zn_{30}$ alloy. This result is supported by the larger negative excess volume for the Mg-Cu alloy (−10%) compared to that of the Mg-Zn alloy (−5.3%), and furthermore by the larger difference of the electro-negativities of Mg and Cu.

For the case of Mg-Cu it was shown that the arrangement of nearest neighbours around a central copper atom is similar in amorphous $Mg_{85.5}Cu_{14.5}$ and in the crystalline phase Mg_2Cu.

Acknowledgements

We kindly acknowledge that part of this work was supported by the Deutsche Forschungsgemeinschaft. One of us (E.N.) also acknowledges financial support by the Deutsche Akademische Austauschdienst and the Max-Planck-Gesellschaft.

[1] N. Shiotani, H. Narumi, H. Arai, K. Wakatsuki, Y. Sasa, and T. Mizoguchi, Proc. 4th Int. Conf. Rapidly Quenched Metals, Sendai 1981, p. 667.
[2] J. Hafner, Proc. 4th Int. Conf. on Rapidly Quenched Metals, Sendai 1981, p. 1311.
[3] C. N. J. Wagner, J. Non. Cryst. Sol. **31,** 1 (1978).
[4] T. E. Faber and J. M. Ziman, Phil. Mag. **11,** 153 (1965).
[5] A. B. Bhatia and D. E. Thornton, Phys. Rev. **B 2,** 3004 (1970).
[6] T. R. Anthony and H. E. Cline, J. Appl. Phys. **50** (1), 239 (1979).
[7] K. Shirakawa, Y. Waseda, and T. Masumoto, Sci. Rep. Ritu, **A 29,** 229 (1981).
[8] W. Hume Rothery and G. V. Raynor, The Structure of Metals and Alloys, Inst. Metals, London 1954.
[9] H. Küstner, Z. Physik **70,** 325 and 468 (1931); **77,** 52 (1932).
[10] R. W. James, The Optical Principle of the Diffraction of X-rays, G. Bell and Sons LTD, London 1958.
[11] J. Krogh Moe, Acta Cryst. **9,** 951 (1956).
[12] D. T. Cromer, Acta Cryst. **18,** 17 (1965); D. T. Cromer and J. T. Waber, Acta Cryst. **18,** 104 (1965).
[13] K. Sagel, Tabellen zur Röntgenstrukturanalyse, Springer-Verlag, Berlin 1958, p. 152.
[14] H. H. Paalmann and C. J. Pings, J. Appl. Phys. **33,** 2635 (1962).
[15] V. F. Sears, Adv. Phys. **24,** 1 (1975).
[16] L. Koester, Neutron Physics, Springer Tracts in Modern Physics **80,** 1 (1977).
[17] G. E. Bacon, Neutron Diffraction, 3rd ed., Oxford 1975.
[18] N. W. Ashcroft and D. C. Langreth, Phys. Rev. **156,** 685 (1967).
[19] P. Scherrer, Natur. Ges. Wiss. Göttingen 1918, p. 98.
[20] K. Schubert and K. Anderko, Z. Metallkunde **12,** 321 (1951).